

## **Role of Microstructure in Promoting Fracture and Fatigue Resistance in Mo-Si-B Alloys**

**J. J. Kruzic**

Department of Mechanical Engineering, Oregon State University, Corvallis, OR 97331, U.S.A.

**J. H. Schneibel**

Oak Ridge National Laboratory, Metals and Ceramics Division, Oak Ridge, TN 37831, U.S.A.

**R. O. Ritchie**

Department of Materials Science and Engineering, University of California, and Materials Sciences Division, Lawrence Berkeley National Laboratory, Berkeley, CA 94720, U.S.A.

### **ABSTRACT**

An investigation of how microstructural features affect the fracture and fatigue properties of a promising class of high temperature Mo-Si-B based alloys is presented. Fracture toughness and fatigue-crack growth properties are measured at 25° and 1300°C for five Mo-Mo<sub>3</sub>Si-Mo<sub>5</sub>SiB<sub>2</sub> containing alloys produced by powder metallurgy with  $\alpha$ -Mo matrices. Results are compared with previous studies that used intermetallic matrix microstructures to determine the role of microstructural variables. It is found that increasing the  $\alpha$ -Mo phase volume fraction (17 – 49%) or ductility benefits the fracture resistance, while  $\alpha$ -Mo matrix materials show improvements over intermetallic matrix alloys. Fatigue thresholds also improved until a transition to more ductile fatigue behavior occurred with large amounts of  $\alpha$ -Mo phase (49%) and ductility (i.e., at 1300°C). The beneficial role of such microstructural variables are attributed to the promotion of the observed toughening mechanisms of crack trapping and bridging by the relatively ductile  $\alpha$ -Mo phase.

### **INTRODUCTION**

Intermetallic based Mo-Si-B alloys have been targeted for high temperature turbine engine applications as potential replacements for nickel based superalloys. Two specific Mo-Si-B alloy systems developed by Akinc *et al.* [1-4] and Berczik [5,6] have received recent attention. While the former is composed entirely of intermetallic compounds, the latter utilizes the relatively ductile  $\alpha$ -Mo phase to impart some ductility and fracture resistance to a three phase microstructure also containing Mo<sub>3</sub>Si and Mo<sub>5</sub>SiB<sub>2</sub> (T2). For any of these alloys to be successful, adequate resistance to oxidation, creep, fracture, and fatigue must be achieved; however, it is recognized that microstructural features which promote improvements in one property are often detrimental to others [7,8]. For example, while a continuous  $\alpha$ -Mo matrix with high volume fraction may be beneficial to the fracture and fatigue behavior [9], this tends to compromise the oxidation and creep resistance [7,8,10-12]. Accordingly, a thorough understanding of how microstructure affects each property is needed so that appropriate trade-offs can be made in the optimization of these alloys. Thus, the present paper seeks to mechanistically understand the specific role of microstructure in determining the fracture and fatigue resistance of alloys based on the  $\alpha$ -Mo, Mo<sub>3</sub>Si, and T2 phases so that educated decisions can be made when optimizing the properties of this exciting new class of high temperature structural materials.

## EXPERIMENTAL DETAILS

Ground powders of composition Mo-20Si-10B (at.%) containing  $\text{Mo}_3\text{Si}$  (cubic A15 structure) and  $\text{Mo}_5\text{SiB}_2$  (tetragonal D8<sub>1</sub> structure) intermetallic phases were vacuum-annealed to remove silicon from the surface and leave an  $\alpha$ -Mo coating on each particle. These were hot-isostatically pressed in evacuated Nb cans for 4 hr at 1600°C and 200 MPa pressure giving final compositions with 7-15 at.% Si and 8-11 at.% B (balance Mo). Five alloys were produced differing in volume fraction of the  $\alpha$ -Mo matrix (17 – 49%) and initial coarseness of the intermetallic particles, fine  $\leq 45 \mu\text{m}$ , medium 45-90  $\mu\text{m}$ , and coarse 90-180  $\mu\text{m}$  (Figure 1). Alloys are designated as F34, M34, C17, C46, and C49, with the letter indicating the microstructural coarseness and the number giving the  $\alpha$ -Mo volume fraction.

Resistance-curve (R-curve) fracture-toughness experiments were performed on fatigue pre-cracked, disk-shaped compact-tension DC(T) specimens (width 14 mm; thickness 3 mm). Samples were loaded monotonically in displacement control at  $\sim 1 \mu\text{m}/\text{min}$  until the onset of cracking. At 25°C, periodic unloads ( $\sim 10$ -20% of peak load) were performed to measure the unloading back-face strain compliance, which was used to determine the crack length [13]. 1300°C tests were conducted in gettered argon using (direct-current) electrical potential-drop techniques to monitor crack length [14].

Fatigue-crack growth testing (25 Hz, sine waveform) was performed at 25° and 1300°C in identical environments in general accordance with ASTM Standard E647[15] using computer-controlled servo-hydraulic testing machines at a load ratio  $R$  (ratio of minimum to maximum loads) of 0.1. Crack-growth rates,  $da/dN$ , were determined as a function of the stress-intensity

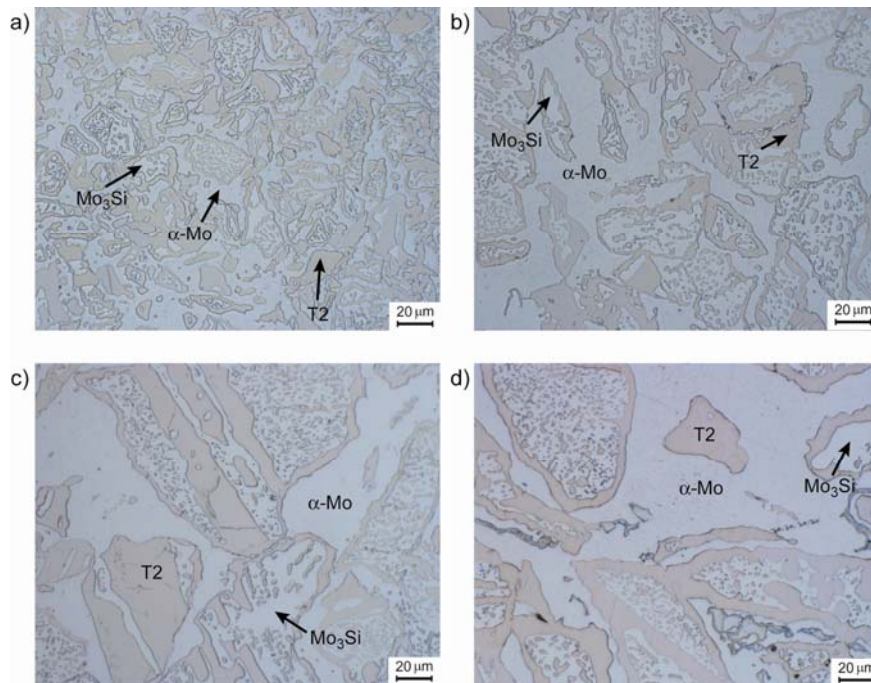


**Figure 1.** Microstructures of alloys (a) F34, (b) M34, (c) C17, and (d) C46. (C49 is seen in Figure 2b)

range,  $\Delta K$ , using continuous load-shedding to maintain a  $\Delta K$ -gradient ( $=1/\Delta K[d\Delta K/da]$ ) of  $\pm 0.08 \text{ mm}^{-1/2}$ .  $\Delta K_{TH}$  fatigue thresholds, operationally defined at a minimum growth rate of  $10^{-10}$ – $10^{-11}$  m/cycle, were approached under decreasing  $\Delta K$  conditions. Both fracture and fatigue testing was periodically paused to observe crack profiles by optical and scanning electron microscopy.

## RESULTS AND DISCUSSION

R-curves for the five Mo-Mo<sub>3</sub>Si-T2 alloys are plotted in terms of the stress intensity,  $K$ , and clearly indicate rising fracture toughness with crack extension (Figure 2a). Furthermore, increasing toughness with higher  $\alpha$ -Mo volume fraction is observed; indeed, alloys C46 and C49 had peak room-temperature toughnesses in excess of 20 MPa $\sqrt{\text{m}}$ , i.e., up to seven times higher than that of monolithic molybdenum silicides [16,17]. Crack trapping and bridging by the  $\alpha$ -Mo phase were identified as the toughening mechanisms responsible for this behavior (Figure 2b), with the effectiveness of these mechanisms rising with increasing  $\alpha$ -Mo content. Experiments at 1300°C on alloys M34, C17, and C46 indicated that the fracture toughness improved at higher temperatures, which was associated with improved  $\alpha$ -Mo ductility. The initiation toughness,  $K_i$ , which defines the beginning of the R-curve, rose ~65% for alloys M34 and C17, while alloy C46 experienced toughening at 1300°C to such a degree that large scale crack blunting and deformation occurred (Figure 3a) and linear-elastic fracture mechanics was no longer a valid method for assessing the toughness using the present specimen size. Thus,  $K_i$  for alloy C46 at 1300°C is reasoned to be significantly larger than the 12.6 MPa $\sqrt{\text{m}}$  measured for alloy M34. Crack blunting was also observed, to a much smaller degree, in the other alloys tested at 1300°C (Figure 3b). Thus, increases in toughness with temperature were attributed to the improved effectiveness of crack trapping due to the enhanced  $\alpha$ -Mo ductility at elevated temperatures.

Fatigue-crack growth results are shown in Figure 4a, from which it is apparent that at 25°C the Paris-law exponents,  $m$ , are extremely high,  $>78$  in all cases, characteristic of brittle

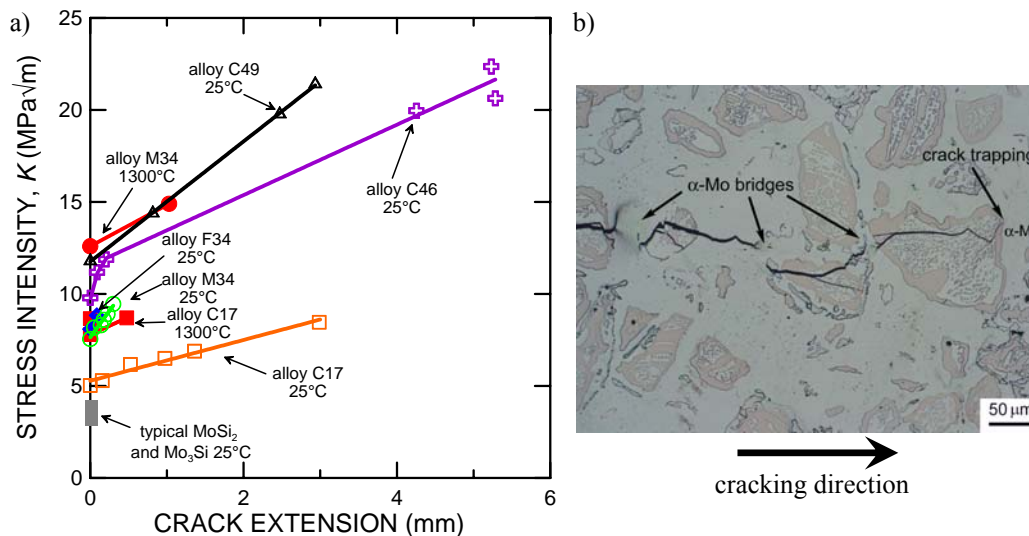


**Figure 2.** (a) shows R-curve behavior for Mo-Si-B alloys, while (b) shows the active toughening mechanisms, crack trapping and bridging by the  $\alpha$ -Mo phase of alloy C49.

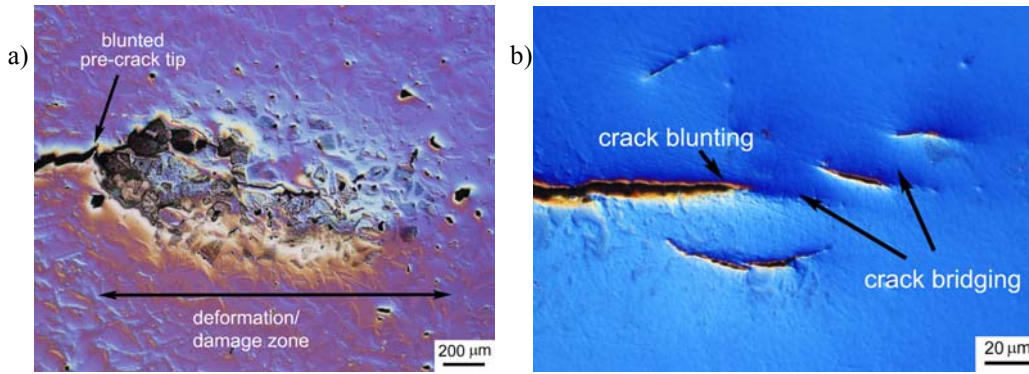


**Figure 3.** Crack blunting seen in alloys (a) C46 and (b) M34 after R-curve testing at 1300°C. Notice the order of magnitude difference in scale between the two micrographs.

materials. Fatigue data was collected for alloys M34 and C49 at 1300°C as well, and although alloy M34 had a similarly high  $\Delta K$  dependence at 1300°C, alloy C49 displayed a transition to more ductile fatigue behavior, with more than an order of magnitude decrease in the Paris-law exponent from 78 to 4. A Paris exponent of 4 is similar to what is expected for ductile metals, which typically have  $m = 2 - 4$  [18].  $\Delta K_{TH}$  thresholds ranged between 5 and 9.5 MPa $\sqrt{m}$  for the five alloys at 25°C (Figure 4a). At 1300°C, due to experimental difficulties and limited numbers of samples, data were not collected near the operationally-defined fatigue threshold; however, based on extrapolation of the data in Figure 4a, the threshold for M34 is expected to be similar to that at 25°C, whereas data for alloy C49 suggests a decrease in the fatigue threshold at 1300°C.

Figure 4b compiles the present fracture and fatigue results along with those for intermetallic matrix Mo-Si-B alloys with similar compositions [19,20]. Here the fatigue thresholds are plotted as the maximum stress intensity,  $K_{max,TH}$ , along with the initiation toughness values,  $K_I$ . Peak

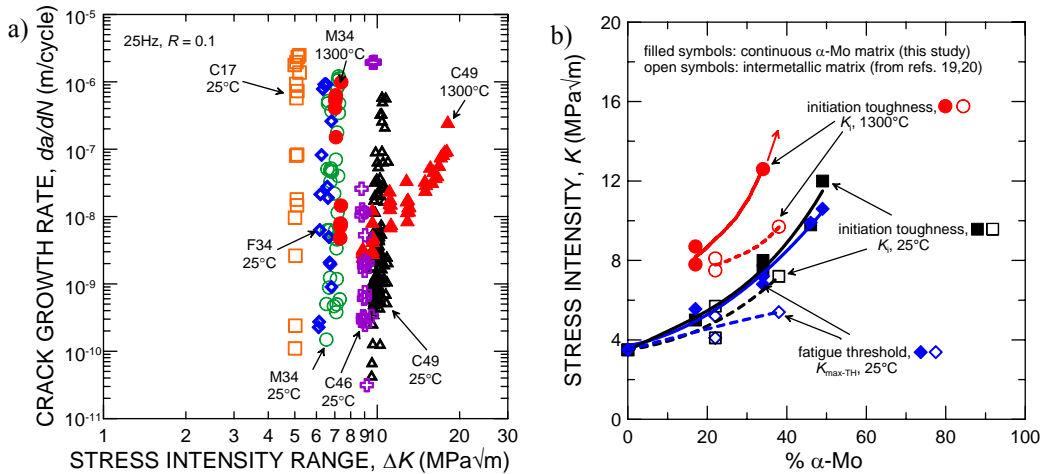


**Figure 4.** (a) shows the fatigue crack growth behavior for present alloys, while (b) plots the fracture and fatigue properties of both the present  $\alpha$ -Mo matrix alloys along with intermetallic matrix alloys from refs. [19,20].

toughnesses are not compared since steady-state, or plateau, values were not achieved due to inadvertent failure of specimens and/or limited specimen size. Figure 4b clearly illustrates that the fracture and fatigue properties of all the alloys improve with increasing  $\alpha$ -Mo volume fraction. Furthermore, the fracture properties are seen to improve with increasing  $\alpha$ -Mo ductility, as evidenced by the higher toughness values at 1300°C for all the alloys. Note that a given toughness value may be achieved with lower  $\alpha$ -Mo volume fraction if the ductility is improved, here this is accomplished by increasing the temperature. Thus, if the room temperature ductility of the  $\alpha$ -Mo phase is improved, lower  $\alpha$ -Mo volume fractions will be needed to achieve adequate toughness levels; this is important since the  $\alpha$ -Mo phase compromises the oxidation and creep resistance [7,8,10-12] and thus its volume fraction should be minimized if possible.

The fracture and fatigue properties are also improved for the  $\alpha$ -Mo matrix materials relative to the intermetallic matrix materials from [19,20]. This is attributed to higher effectiveness of the crack trapping and bridging mechanisms when there is a continuous  $\alpha$ -Mo matrix, since the crack cannot avoid the relatively ductile phase. Although this appears to have weaker influence when compared to  $\alpha$ -Mo volume fraction and ductility, the effect is enhanced when either of those microstructural variables is increased, indicating that these microstructural variables do not affect the mechanical behavior independently. Finally, alloys with coarser microstructural scale demonstrated slightly improved fracture and fatigue behavior. This may be seen in the improved crack stability for alloy C17 relative to the tougher alloys F34 and M34. Although F34 and M34 were tougher due to higher  $\alpha$ -Mo volume fractions, stable crack growth was more easily accomplished in alloy C17, allowing the collection of R-curve data over several millimeters without catastrophic failure.

## CONCLUSIONS

Based on experimental ambient- to high-temperature fracture toughness and fatigue-crack propagation results for five Mo-Si-B alloys, containing  $\text{Mo}_3\text{Si}$  and  $\text{Mo}_5\text{SiB}_2$  intermetallic phases dispersed within a continuous  $\alpha$ -Mo matrix, the following conclusions are made:

1.  $\alpha$ -Mo matrix Mo-Si-B alloys exhibit far superior fracture and fatigue resistance relative to unreinforced silicides, with fracture toughnesses in excess of  $20 \text{ MPa}\sqrt{\text{m}}$  for  $\alpha$ -Mo volume fractions  $> 45\%$ . Such gains are attributed to crack trapping and crack bridging by the  $\alpha$ -Mo phase.
2. Higher  $\alpha$ -Mo volume fractions benefited both of these mechanisms, leading to improved fracture and fatigue resistance. Furthermore, fracture resistance was improved at 1300°C, indicating the role that  $\alpha$ -Mo ductility plays in determining mechanical properties. Finally, a given level of fracture resistance may be achieved with lower  $\alpha$ -Mo volume fraction by improving  $\alpha$ -Mo ductility, a desirable feature since  $\alpha$ -Mo compromises the oxidation and creep resistance.
3. Using a continuous  $\alpha$ -Mo matrix instead of an intermetallic matrix is also beneficial for the fracture and fatigue properties; however, not as much so as  $\alpha$ -Mo volume fraction and ductility. Additionally, coarser microstructural scale also benefits the fracture and fatigue behavior, specifically by aiding bridging and crack stability.
4. Successful Mo-Si-B materials will need to optimize the microstructure for several mechanical properties and the oxidation resistance. The present results identify the role

of various microstructural variables in determining the fracture and fatigue properties, which can be utilized to aid in the design of future alloys.

## ACKNOWLEDGEMENTS

Work supported by the Office of Fossil Energy, Advanced Research Materials Program, WBS Element LBNL-2, and by the Office of Science, Office of Basic Energy Sciences, Division of Materials Sciences and Engineering of the U.S. Department of Energy, under contract DE-AC03-76SF0098 with the Lawrence Berkeley National Laboratory for ROR and JJK. JHS acknowledges funding of this work by the Office of Fossil Energy, Advanced Research Materials (ARM) Program, WBS Element ORNL-2(I), U.S. Department of Energy, under contract DE-AC05-00OR22725 with Oak Ridge National Laboratory managed by UT-Battelle.

Deleted: , and by the Division of Materials Sciences and Engineering,

## REFERENCES

1. M. K. Meyer, M. J. Kramer, and M. Akinc, *Intermetallics* **4**, 273 (1996).
2. M. K. Meyer and M. Akinc, *J. Am. Ceram. Soc.* **79** (10), 2763 (1996).
3. M. K. Meyer, A. J. Thom, and M. Akinc, *Intermetallics* **7**, 153 (1999).
4. M. Akinc, M. K. Meyer, M. J. Kramer, A. J. Thom, J. J. Heubsch, and B. Cook, *Mater. Sci. Eng.* **A261** (1-2), 16 (1999).
5. D. M. Berczik, United States Patent No. 5,595,616 (1997).
6. D. M. Berczik, United States Patent No. 5,693,156 (1997).
7. J. H. Schneibel, R. O. Ritchie, J. J. Kruzic, and P. F. Tortorelli, *Metall. Mater. Trans. A*, in press (2004).
8. J. H. Schneibel, P. F. Tortorelli, M. J. Kramer, A. J. Thom, J. J. Kruzic, and R. O. Ritchie, in *Defect Properties and Related Phenomena in Intermetallic Alloys*, edited by E. P. George, M. J. Mills, H. Inui, and G. Eggeler (Materials Research Society, Warrendale, PA, 2003), Vol. 753, pp. 53-58.
9. J. J. Kruzic, J. H. Schneibel, and R. O. Ritchie, *Scripta Mater.* **50**, 459 (2004).
10. J. H. Schneibel, C. T. Liu, D. S. Easton, and C. A. Carmichael, *Mater. Sci. Eng.* **A261** (1-2), 78 (1999).
11. V. Supatarawanich, D. R. Johnson, and C. T. Liu, *Mater. Sci. Eng.* **A344** (1-2), 328 (2003).
12. J. H. Schneibel, *Intermetallics* **11** (7), 625 (2003).
13. C. J. Gilbert, J. M. McNaney, R. H. Dauskardt, and R. O. Ritchie, *J. Test. Eval.* **22** (2), 117 (1994).
14. D. Chen, C. J. Gilbert, and R. O. Ritchie, *J. Test. Eval.* **28** (4), 236 (2000).
15. ASTM E647-00 in *Annual Book of ASTM Standards, Vol. 03.01: Metals- Mechanical Testing; Elevated and Low-temperature Tests; Metallography* (ASTM, West Conshohocken, Pennsylvania, USA, 2002), pp. 595-635.
16. K.T. Venkateswara Rao, W. O. Soboyejo, and R. O. Ritchie, *Metall. Trans.* **23A**, 2249 (1992).
17. I. Rosales and J. H. Schneibel, *Intermetallics* **8**, 885 (2000).
18. R. O. Ritchie, *Int. J. Fract.* **100** (1), 55 (1999).
19. H. Choe, D. Chen, J. H. Schneibel, and R. O. Ritchie, *Intermetallics* **9**, 319 (2001).
20. H. Choe, J. H. Schneibel, and R. O. Ritchie, *Metall. Mater. Trans.* **34A**, 25 (2003).